Estimation of actual evapotranspiration over a rainfed vineyard using a 1-D water transfer model: A case study within a Mediterranean watershed

Mauricio Galleguillos, Frédéric Jacob, Laurent Prevot, Carlos Faúndez, Aline Bsaibes

Estimation of actual evapotranspiration over a rainfed vineyard using a 1-D water transfer model: A case study within a Mediterranean watershed

Mauricio Galleguillos [a, b, *], Frédéric Jacob [c], Laurent Prévot [d], Carlos Faúndez [e], Aline Bsaibes [f]

[a] Faculty of Agronomic Sciences, University of Chile, Santiago, Chile
[b] Center for Climate Resilience Research (CR2), University of Chile, Santiago, Chile
[c] IRD/UMR LISAH (INRA, IRD, SupAgro), Montpellier, France
[d] INRA/UMR LISAH (INRA, IRD, SupAgro), Montpellier, France
[e] Soil Physics and Land Management Group, Wageningen University, Wageningen, The Netherlands [f] ITK, Montpellier, France

Keywords: Heterogeneous landscape; HYDRUS-1D; Vadose zone Water table

Abstract

The current study aims to evaluate the capabilities of soil water balance modeling to estimate ET for very different conditions of rainfed grapevine water status, within a vineyard landscape that depicts heterogeneities in canopy, soil and water table conditions. We calibrated the HYDRUS-1D model against measurements of the soil moisture profile within seven contrasted sites, we validated HYDRUS-1D simulations against ET estimates derived from eddy covariance (EC) measurements within two contrasted sites, and we analyzed the temporal dynamics of the HYDRUS-1D ET simulations throughout almost two growth cycles for the seven sites. The calibration of HYDRUS-1D was correctly achieved, with a relative RMSE of 20% on average. Validation of HYDRUS-1D simulations against EC measurements was satisfactory, with RMSE values of about 40 W m^{-2} at the hourly timescale and 0.5 mm d^{-1} at the daily timescale. HYDRUS-1D was able to provide consistent time series of ET within the seven contrasted sites and throughout the two growth cycles. We conclude that HYDRUS-1D simulations can be used as an alternative to EC measurements within rainfed vineyards, to alleviate experimental efforts for device cost and maintenance. Further, HYDRUS-1D simulations can be used for characterizing spatial variabilities and temporal dynamics, assessing impact of pedological conditions and land use on ET, or validating remote sensing retrievals over regional extents.

1. Introduction

For ages, grapevine (Vitis Vinifera L.) has been an important rainfed monoculture in Mediterranean regions, occupying large areas that have mostly extended over France, Italy and Spain (OIV, 2007). Mediterranean grapevine monoculture has direct implications in terms of land use, jobs and incomes (Lereboullet et al., 2013). Nowadays, water use in Mediterranean regions is characterized by increasing competition between different purposes, which can affect wine growing through groundwater availability. Meanwhile, the competition may be sharpened under the influence of global warming (Tóth and Végvári, 2016).

The grapevine organoleptic properties depend upon root zone soil moisture. Under unrestrictive water availability, grapevine can generate excessive vegetative growth that competes with assimilate accumulation within grapes. This process induces an excess of canopy vigor, generating in turn changes in the fruit zone microclimate with an increase in humidity and disease occurrence (Smart, 1973; Zahavi et al., 2001; Pellegrino et al., 2006; Liang et al., 2014). Conversely, grapevine can experience severe water stress for long periods in summer, when evaporative demand is maximal and rainfall is negligible. In such situations, root zone moisture is strongly reduced, and assimilate production decreases with grape yield and quality (Pellegrino et al., 2005; Griesser et al., 2015). These processes underline the necessity to quantify grapevine water status throughout the growing cycle, in order to improve grape production and water resource management within vineyard landscapes.

Quantifying grapevine water status requires knowledge of actual evapotranspiration (ET) that directly drives both surface soil moisture through soil evaporation and root zone soil moisture through plant transpiration (Montes et al., 2014). However, estimating vineyard evapotranspiration is challenging because of the architectures of aboveground canopy and subsurface root system that are typified by trellis and row structures. Thus, it is necessary to discriminate soil evaporation and plant transpiration (Heilman et al., 1994; Kool et al., 2014a), to account for shadow effects in accordance to sun position and row orientation (Riou et al., 1994; Heilman et al., 1996; Zarco-Tejada et al., 2005), and to pay attention to the combined effect of wind direction and canopy geometry (Heilman et al., 1994; Zhang et al., 2008; Ortega-Farias et al., 2010).

Nowadays, ET measurements over land surfaces commonly rely on the eddy covariance (EC) method (Zitouna-Chebbi et al., 2012, 2015). The EC method has been successfully used over irrigated and rainfed vineyards (Li et al., 2008, 2009; Galleguillos et al., 2011a, 2011b; Kool et al., 2014a; Montes and Jacob, 2016) while some studies relied on other micro-meteorological methods such as the Bowen ratio-energy balance (Heilman et al., 1994; Spano et al., 2000; Yunusa et al., 2004; Zhang et al., 2008). Overall, most of the existing studies involved long-term experiments, and provided important outcomes for better understanding the temporal dynamics of ET throughout the grapevine growth cycle. However, the use of micrometeorological methods is limited by experimental efforts in terms of device cost and maintenance, especially when addressing heterogeneous landscapes that require networks of measurement plots across areas spreading over several square-kilometers.

Another way to estimate ET consists of using mechanistic models based on the resolution of mass and energy balances, along with in-situ measurements of ET drivers such as

micrometeorological variables or soil moisture (e.g., Verstraeten et al., 2008; Kool et al., 2014b). Existing studies for irrigated and rainfed vineyards relied on the Penman-Monteith formalism and its extensions to dual and multiple source modeling (Sene, 1994; Ortega-Farias et al., 2007, 2010; Zhang et al., 2008), possibly including the coupling with a soil water balance to address the growth cycle (Montes et al., 2014). These studies reported good performances for the proposed approaches, but some of them underlined the restricted applicability to other conditions, mainly because of changes in soil hydrodynamic and canopy aerodynamic properties. The proposed approaches either excluded the soil water balance or describe it very coarsely, without paying much attention to water fluxes within the unsaturated zone and especially to capillary rises caused by water table fluctuations. A first attempt to address water fluxes within the unsaturated zone was conducted by Kool et al. (2014a), but the study focused on soil evaporation in an arid area without water table fluctuation.

As compared to either direct measurements based on the EC method or to indirect measurements based on energy balance modeling, the use of water balance modeling is an alternative for the monitoring of ET within heterogeneous vineyards. First, it does not require elaborated information about aerodynamic properties. Second, it permits the consideration of water table fluctuations that strongly drive the functioning of grapevine within rainfed vineyards (Guix-Hébrard et al., 2007). Third, it relies on measurements of the soil moisture profile to calibrate model parameters related to soil properties, thus alleviating experimental efforts in terms of device cost and maintenance. Indeed, measurements of the soil moisture profile can be replicated across large spatial extents by using reliable techniques such as time domain reflectometry (TDR) or neutron probe (NP), as reviewed by Dobriyal et al. (2012).

The purpose of the current study was to evaluate the capabilities of soil water balance modeling to estimate ET for contrasted conditions of grapevine water status, within a vineyard landscape that depicts heterogeneities in terms of canopy, soil and water table conditions. For this, we evaluated the calibration of a soil water balance model over in-situ measurements of the soil moisture profile, we validated the model simulations against independent EC measurements, and we analyzed the model simulations at hourly and daily timescales throughout the grapevine growth cycle. The paper is structured as follows. We first detail the materials and methods, including the study area and the in-situ measurements (Section 2), as well as the estimation of ET by means of EC measurements and of soil water balance modeling (Section 3). We second report the calibration results (Section 4.1), the validation results (Section 4.2), and the analysis of the temporal dynamics for simulated ET throughout the growth cycle (Section 4.3). We third discuss the results in the light of previous studies (Section 5), and we finally conclude on both the study outcomes and the future challenges.

2. Materials and data

We calibrated the soil water balance model against soil moisture measurements, and we analyzed the model simulations over seven sites that depicted a gradient in grapevine water status. We validated the soil water balance model against EC measurements for two sites amongst the seven, where the two sites depicted very contrasted grapevine water status. We present hereafter the data collection within these seven sites.

2.1. Study site: the Peyne watershed

The study took place within the Peyne watershed that is located in the Languedoc-Roussillon region of southern France (43.49°N, 3.37° E, 80 m asl). The area is mainly devoted to vine growing (70%) while cereals, alfalfa and scrublands constitute the main additional land uses. Annual rainfall ranges from 400 to 1300mm, distributed in autumn and spring with large inter-annual variability. Annual ET obtained with the Penman-Monteith method (Allen et al., 1998) is close to 1100mm (Trambouze and Voltz, 2001). Over the [1993–2015] period, averaged values of annual rainfall and annual ET were 634 mm and 1110 mm, respectively.

Vineyards are located over relatively flat terrains with a 4% slope on average, whereas 90% of these terrains have slopes less than 10%. Soils depict large heterogeneities in texture, depth and parent material, which leads to very different conditions in terms of soil moisture and rooting depth. Additionally, water table within the rooting zone depict a large range of conditions, including absent, transient or permanent water tables during the growth cycle. Overall, both soil and water table conditions induce very contrasted situations in terms of grapevine water status.

2.2. Experimental plots and calendar

We assessed the capabilities of soil water balance modeling to estimate ET over seven sites, features of which are listed in Table 1. The seven sites had similar trellis structures, with averaged values of 2.5 m, 1 m and 1.5 m for row spacing, max row width and canopy height, respectively. Sites 1–5 and 7 corresponded to one field, with size ranging from 0.03 to 0.09km^2. Site 6 had a 0.15 km^2 size, and spread over nine fields including vineyards by 90% in surface area. The experiment lasted from August 2007 (middle of growing season) to October 2008 (end of harvest period).

Table 1. Characteristics of the seven sites selected within the Peyne watershed. The "Devices" column indicates the (1) number of locations within each site for measuring soil moisture profiles with NP and TDR devices, and (2) the collection of eddy covariance (EC) measurements when applicable. A soil was considered shallow when the underlying parental material was above a 2.5-m depth. Each location of NP data was equipped for piezometric measurements. Water table conditions are related to winter and spring seasons. An absent water table (respectively permanent water table) means a piezometric level below (respectively above) the 2.5-m depth throughout the year. A seasonal water table means a piezometric level above the 2.5-m depth during winter and spring.

Site number	Devices	Soil Depth	Soil texture	Water table conditions	Size (m^2)	Variety
1	1 NP	Shallow	Sandy, Silty	Absent	32701	Syrah
2	1 NP	Shallow	Clay, Gravels	Seasonal	74966	Grenache blanc
3	2 NP	Shallow	Silty, Sandy	Absent	29894	Cabernet Franc
4	1 NP	Deep	Clay loam	Permanent	53851	Cabernet Sauvignon
5	2 NP	Deep	Clay	Seasonal	81052	Merlot
6	9 NP, EC	Deep/Shallow	Silty, Clay loam	Seasonal	145825	Syrah/Cabernet Sauvignon
7	1 NP, EC	Deep	Clay	Absent	92312	Cabernet Sauvignon

2.3. Data collection and related devices

To constrain the soil water balance model on atmospheric forcing, hourly values of air temperature and relative humidity, wind speed, solar irradiance and rainfall were collected within Site 6 with a CIMEL ENERCO 400 station (CIMEL Electronics, Paris, France) by following meteorological standards apart from wind speed (measured at 2 m height rather than 10 m). These hourly meteorological data were further used to estimate short-grass

reference evapotranspiration (ET_0) by means of the Penman approach for standard conditions (Valiantzas, 2006).

To constrain the soil water balance model on water fluxes within the unsaturated zone, the seven sites were monitored bi-weekly and after each event of heavy rainfall for the soil moisture profiles and the water table level. Vegetation canopy structure was also monitored regularly. The data collection was conducted around solar noon, and it included three items. First, soil moisture profiles were sampled every 0.2 m to the 2.5-m depth with a Vectra 503-DR CPN neutron probe (NP) (Vectra, la Verrière, France), and completed for the upper 0.15 m using a Soil Moisture Equipment TRASE 6050 time domain reflectometry (TDR) sensor (Soil Moisture Equipment Corp., Santa Barbara, CA). The number of locations for collecting soil moisture profiles (Table 1) varied according to site size and soil heterogeneity derived from a pedological map. For each location, we beforehand characterized thickness and texture for soil horizons by using in-situ observations along with expert knowledge, and we ascertained soil surface properties using additional archive information from former studies in the same region (Trambouze and Voltz, 2001; Bsaibes, 2007). Second, the water table level was monitored to the 2.5-m depth with manual piezometric devices. The monitoring was continuous on Site 6 and regular on the other sites for which the two-week frequency observations were linearly interpolated. Third, vegetation structures were monitored for grapevine canopy structure (height, thickness and width), over one (Site 1–5 and 7) or more (Site 6) fields. Following Trambouze (1996), the monitoring was conducted in winter and summer, and next interpolated at the daily timescale. Row orientation and spacing were measured once.

To validate the soil water balance model simulations, EC devices were set up for direct ET measurements within two sites that differed much in canopy structure, soil hydrodynamic properties and water table dynamics. We set up a temporary flux station on Site 7, whereas a permanent flux tower was installed on Site 6 in the context of the environmental research observatory OMERE (a French acronym for the Mediterranean Observatory of Water and the Rural Environment, http://www.umr-lisah.fr/omere). To measure wind speed components and air temperature, each flux station was equipped with a R.M. Young 81000 3D sonic anemometer (R.M. Young Co., Traverse City, MI, USA). To measure air humidity, the flux station on Site 6 was equipped with a LiCor LI7500 fast hygrometer (LiCor Inc., Lincoln, NE, USA), and the flux station on Site7 was equipped with a Campbell KH2O fast hygrometer (Campbell Scientific Co., USA). For Site 6 (respectively Site 7), that included nine (respectively one) fields, the sensors were setup 6.2 m (respectively 2.5 m) above ground, and the acquisition frequency was set to 20 Hz to avoid spectral loss for wind speed values up to 6 m s^{-1} (respectively 3 m s^{-1}).

All instruments were manufacturer-calibrated. The NP was calibrated by accounting for soil type and moisture. Calibration was performed against gravimetric soil moisture data at each depth of NP measurement (soil density was estimated using a Campbell DR 501 gamma probe, Campbell Scientific Co., USA), and the calibration residual error was 0.04 m3 m^{-3} (15% relative).

3. Methods: estimating actual evapotranspiration (ET)

3.1. Direct estimation from eddy covariance measurements

For Site 6 and 7, sensible and latent heat fluxes were calculated at the hourly timescale from the EC measurements. The latter were preprocessed by applying the whole set of instrumental corrections proposed by the ECPACK version 2.5.20 library (van Dijk et al., 2004) along with the double rotation correction (Kaimal and Finnigan, 1994). Fluxes were calculated along with tolerance intervals, about 20% and 12% for Sites 6 and 7, respectively. For energy balance closure, the sum of convective fluxes and available energy agreed within 80% for Site 7. Daily ET was finally calculated as the sum of hourly ET.

We evaluated the daytime footprints of the EC measurements using the approach proposed by Horst and Weil (1992) for scalar fluxes. We calculated the footprints as ellipsoids located a few meters from which 90% of the convective fluxes originated. For site 7 that was a homogenous vineyard, the footprint extensions always remained within the field, and the EC station was located few meters far from the neutron probe (NP) access tube. For site 6 that included nine vineyard fields, a sensitivity analysis showed that the footprints had a median size of 0.12 km^2 and thus included the nine neutron probe access tubes (Bsaibes, 2007).

3.2. Indirect estimation from HYDRUS-1D model simulations

For each of the seven sites within the Peyne watershed, ET was indirectly estimated by calibrating a soil water balance model over time series of soil moisture profiles measured with NP and TDR devices. We choose the HYDRUS-1D model (Simunek et al.,2016) as the soil water balance model, because it includes the state of the art for water and solute movements in the vadose zone. HYDRUS1D has been widely used for various agricultural studies, including water and nitrogen fluxes under different crops (Ramos et al., 2012; Phogat et al., 2013), water fluxes and wetting patterns under drip irrigation (Patel and Rajput,2008; Kandelous and Simunek,2010; Kandelous et al., 2012; Arbat et al., 2013; Kool et al., 2014a), solute transports under saline irrigation (Ramos et al., 2011), or water, salinity and nitrate dynamics under drip irrigation (Phogat et al., 2014). HYDRUS-1D includes several options for upper and lower boundary conditions, to address various conditions. Water fluxes and solute transport are solved using the Richards equation and the advective-dispersive equation, respectively.

For each of the seven sites within the Peyne watershed, HYDRUS-1D was calibrated over the soil moisture profiles measured between August 2007 and October 2008, by constraining the model simulation over a single period that spread from the beginning of March 2007 to the beginning of October 2008. We started the simulation period a few months before the experimental period so that the simulation process was numerically leveled off when calibrating HYDRUS-1D simulations with the measured soil moisture profiles. We detail hereafter the implementation of HYDRUS-1D, including the forcing and calibration strategies, as well as the obtaining of model simulations for soil water balance and ET at the hourly and daily timescale.

3.2.1. Water flux and domain discretization

HYDRUS-1D simulates water fluxes within the unsaturated zone by using the Richards equation in one dimension (Richards, 1931).

$$\frac{\partial \theta}{\partial t} = \frac{\partial}{\partial z}\left[K(h)\left(\frac{\partial h}{\partial z} + 1\right)\right] - S(h) \qquad (1)$$

where θ is volumetric water content ($m^3\ m^{-3}$), h is soil water potential also called pressure head (m), t is time (s), z is vertical ascending coordinate (m), K is unsaturated hydraulic conductivity ($m\ s^{-1}$), and S(h) is water uptake by roots ($m^3\ m^{-3}\ s^{-1}$). For each horizon, retention curve θ (h) and unsaturated hydraulic conductivity K (h) were characterized using the van Genuchten functions (van Genuchten, 1980):

$$\theta(h) = \begin{cases} \theta r + \dfrac{\theta s - \theta r}{\left(1 + |\alpha h|^n\right)^m} & h < 0 \\ \theta_s & h \geq 0 \end{cases} \quad \text{with} m = 1 - \frac{1}{n}; n > 1 \qquad (2)$$

$$K(h) = K_s Se^{\frac{1}{2}}\left(1 - \left(1 - Se^{\frac{1}{m}}\right)^m\right)^2 \qquad (3)$$

$$\text{with}\ Se(h) = \frac{\theta(h) - \theta r}{\theta s - \theta r} \qquad (4)$$

where these functions depend upon residual (θr) and saturated (θs) soil moisture, saturated hydraulic conductivity Ks, effective water content Se, bubbling pressure α and pore-size distribution index n.

For each soil horizon, values of residual and saturated soil moisture were derived from minimum and maximum soil moisture values measured with the NP and TDR devices throughout the experiment. For topsoil (first horizon), the three other inputs of van Genuchten functions (Ks, α and n) were obtained from previous observations within the Peyne watershed (Trambouze and Voltz, 2001; Bsaibes, 2007). For deeper horizons, these three inputs were determined using the module of HYDRUS-1D inverse mode as a calibration procedure. The latter consists of minimizing, over the simulation period, the differences between simulated and measured profiles of soil moisture. The initial guess for the three inputs were derived either from literature values wherever possible (Trambouze and Voltz, 2001; Bsaibes, 2007), or from the ROSETTA module of HYDRUS-1D otherwise.

We simulated the soil water balance over the soil portion between 0 and 2.5-m depth. We split this soil portion into a limited number of horizons in accordance with in situ observation and expert knowledge (between two and four horizons, including surface), and we next discretized the whole soil portion into 251 layers for numerical simulations.

3.2.2. Boundary conditions

For the upper boundary conditions, meteorological forcing included rainfall, soil potential evaporation Ep, and plant maximal transpiration Tv. Rainfall was measured by the meteorological station (Section 2.3). Tv was adjusted to potential transpiration, which was within the confidence interval reported by Trambouze and Voltz (2001) who suggested a 10% larger value for grapevine. Both Tv and Ep were derived from short-grass reference evapotranspiration (ET_0) using the Riou model designed for grapevine canopies (Riou et al., 1994; Bsaibes, 2007) and previously validated in Site 6 by Trambouze and Voltz (2001). Riou model infers Tv as a fraction of ET_0 by assuming that the ratio Tv/ET_0 equals the ratio Rv of solar irradiance absorbed by grapevine leaves to that absorbed by the whole grapevine canopy:

$$Tv = ET_0 \frac{Rv}{(1 - r)\,Rg} \qquad (5)$$

where Rg is solar irradiance, r is grapevine canopy reflection coefficient over the solar domain, set to 0.2 by following Bsaibes (2007), and Rv is geometrically derived from solar position and canopy structure. Finally, soil potential evaporation is determined as:

$$Ep = ET_0 - Tv = ET_0 \left(1 - \frac{Rv}{(1 - r)\,Rg}\right) \qquad (6)$$

For the lower boundary conditions, we set them to free drainage when the water table was absent, and to variable pressure head at the water table level according to piezometric measurements otherwise.

3.2.3. Root water uptake S(h)

The root density was distributed according to both in situ observations and previous studies (Trambouze and Voltz, 2001; Bsaibes, 2007). The average root profile extended between 0.25 and 2.2 m, with 75% of cumulated root density between 0.25 and 1.25 m. Since HYDRUS-1D could not accommodate horizontal changes in root profile (e.g., below the grapevine rows and the inter-rows), we assumed that the root profile was homogeneous within each site, following Trambouze (1996).

For each soil layer with a given root density, root water uptake S(h) corresponds to the regulation of plant maximal extraction by pressure head. Plant maximal extraction is plant maximal transpiration normalized by the relative root density of the layer (i.e., the ratio of layer root density to total root density). This means that plant maximal transpiration is distributed over the soil layers proportionally to their root density, and is locally controlled according to soil moisture (Simunek and Hopmans,2009).

The regulation of plant maximal extraction is expressed using the Feddes function (Feddes et al., 1978). The latter is a trapezoid-like function with a linearly increasing uptake between h_1 (pressure head below anaerobic conditions without uptake) and h_2 (pressure head at maximum uptake), a plateau with maximum uptake between h_2 and h_3 (pressure head at

maximum uptake), and a linearly decreasing uptake between h3 and h4 (pressure head at wilting point). Following Wesseling (1991), the h1 and h2 parameters were set to −0.001mm and to −0.0025mm, respectively. Following Trambouze and Voltz (2001), h3 and h4 parameters were set to −10000 mm and to −150000 mm, respectively.

3.2.4. Actual evapotranspiration

Actual soil evaporation is derived from soil potential transpiration Ep by using the Neuman conditionality that modulates Ep according to surface pressure head and soil moisture (Neuman et al., 1974). The threshold value for the Neuman conditionality was adjusted to −10190 mm (respectively +10 mm) for the minimum (maximum) soil pressure head that correspond to complete dryness (wetness at runoff initiation).

Actual plant transpiration is estimated as the sum of root water uptake over all layers (Vrugt et al., 2001). Thus, HYDRUS-1D is based on a macroscopic approach that consists of deriving actual plant transpiration through the formulation of root water uptake S(h) in a multiple layer framework.

Finally, actual evapotranspiration was estimated as the sum of actual soil evaporation and actual plant transpiration. Simulated ET values at the hourly timescale were aggregated at the daily timescale. The hourly timescale was related to changes in sunlit and shadow effects within vineyards rows, and the daily timescale was related to dynamics of soil water balance.

4. Results

4.1. Assessing calibration consistency

We first evaluated the consistency of the HYDRUS-1D calibration by analyzing the calibration residual errors, i.e., the differences between the measured and the simulated soil moisture profiles. The analysis was conducted by considering the calibration residual errors as a function of soil depth, the calibration residual error from one site to another and throughout the simulation period, and the differences between measurements and simulations for soil water storage, where the latter was derived from the integration of soil moisture profiles.

Over all dates and all locations of soil moisture profile measurements, the average profile of root mean square error (RMSE) between measured and simulated soil moisture decreased with depth, from 0.06 (top) to 0.03 $m^3 m^{-3}$ (bottom). Similarly, the average profile of relative RMSE (i.e., the ratio of absolute RMSE to observed mean value, labeled RRMSE) decreased from 30% to 10%, with an overall value of 20% (Fig. 1). The largest RMSE and RRMSE values were observed around the 1-m depth that corresponded to the maximum root density. The RMSE and RRMSE profiles varied much from one date to another and from one location to another, with values ranging from 0 to 0.15 $m^3 m^{-3}$ and from 0% to 60%, respectively. The lowest and largest values were observed for Sites 4 and 1, respectively. For all measurement locations, the RMSE and RRMSE values systematically decreased with simulation time.

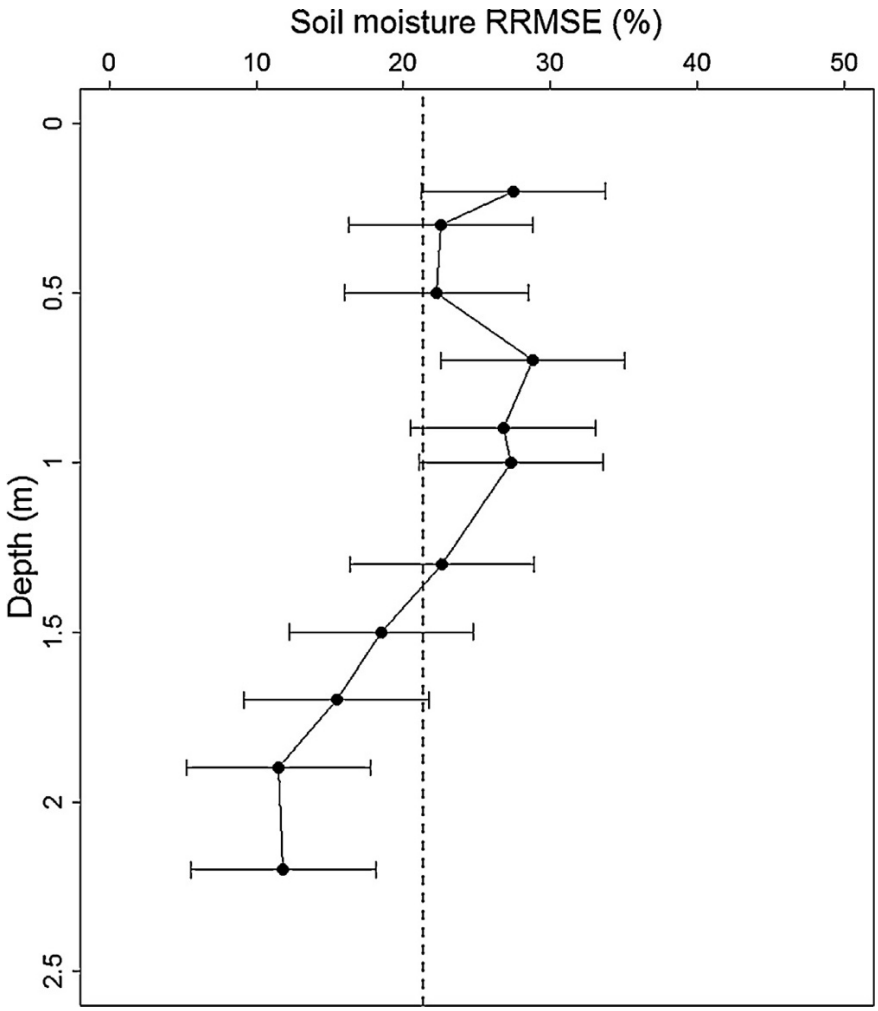

Fig. 1. Profile of HYDRUS-1D residual calibration error, obtained by calculating RRMSE values between measured and simulated soil moisture profiles over all dates and all measurement locations. The dotted line represents the overall mean value, and the error bars represent for each depth the RRMSE standard deviation.

When addressing soil water storage, we observed an overall 10% relative difference between measured and simulated values. Fig. 2 displays a typical example of comparison between measurements and simulations, for two sites that differed much in terms of water availability (i.e., Site 3 was typified by an absent water table and Site 5 was typified by a seasonal water table). As illustrated with the two examples of Fig. 2, the measurements and simulations depicted very similar temporal dynamics, regardless of considered site. We did not identify any systematic over- or under- estimation, neither for a given site throughout the simulation period, nor for a specific period over the seven sites. Fig. 2 indicates that the sites depicted stable soil water storage from January to June 2008, with a peak in June 2008 after heavy rainfall, whereas soil water storage rapidly decreases from July because of both grapevine transpiration and lack of heavy rainfall.

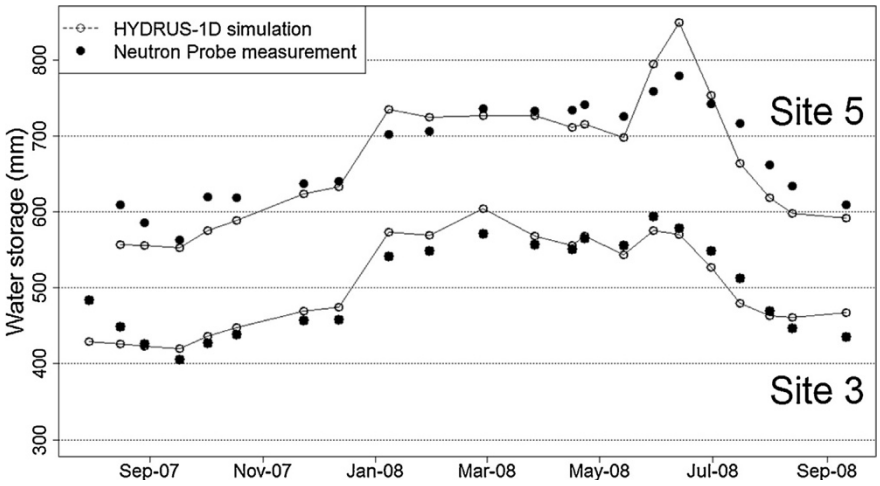

Fig. 2. Comparison of temporal dynamics for measured and simulated soil water storage between August 2007 and October 2008 when considering two contrasted sites. Water storage was calculated by integrating the measured and simulated soil moisture profiles at noon. Site 3 was typified by restrictive water availability because of absent water table, whereas Site 5 was typified by moderate water availability because of a seasonal water table.

4.2. ValidatingHYDRUS-1Destimatesofevapotranspiration against EC measurements

The validation of HYDRUS-1D estimates of evapotranspiration against independent estimates from EC measurements was conducted at both the hourly and daily timescales.

At the hourly time scale, the validation was conducted over daytime hours since nighttime ET is negligible at the daily timescale. When considering the whole simulation period, the RMSE between EC and HYDRUS-1D estimates was 44 W m^{-2} (54% relative) for Site 6 with intermediate water status related to a shallow water table and silty/clay loam soils. For Site 7 with severe water stress in summer because of clay soil along with the lack of a water table, the RMSE was 40 W m^{-2} (44% relative). For both sites, linear regressions between EC and HYDRUS-1D estimates provide slopes and offsets that were close to 1 and 0, respectively, which indicated that systematic errors were very low (Fig. 3). However, we observed large scatters around the regression lines, which indicated that unsystematic errors were large. When analyzing the diurnal course of RRMSE, we observed that the latter was lower between 11 AM to 3 PM for Site 6 (RRMSE<45%) and between 12 AM to 4 PM for Site 7 (RRMSE < 40%).

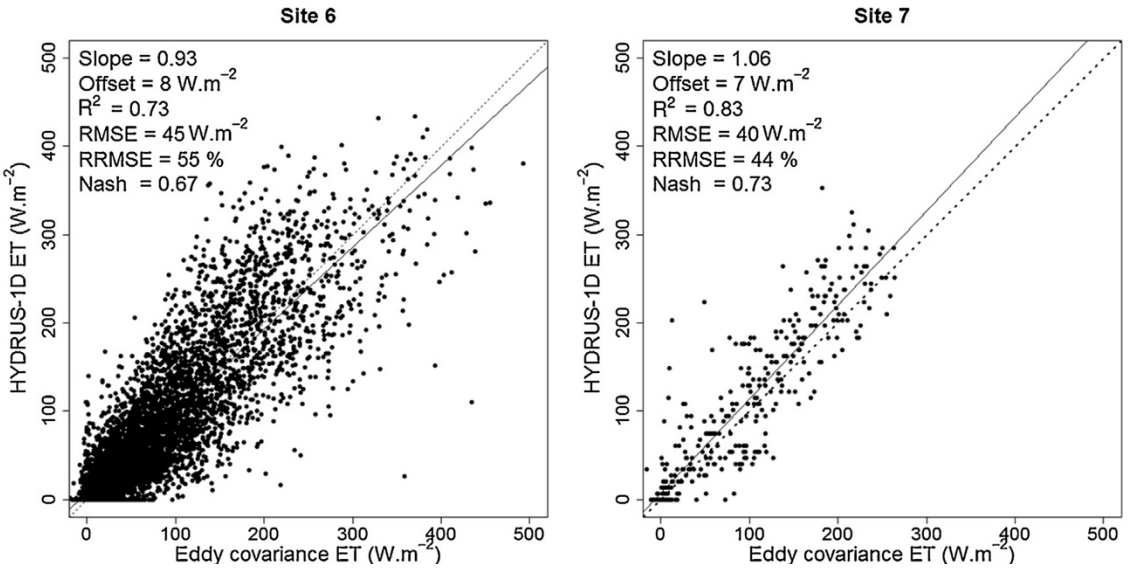

Fig. 3. Validation of HYDRUS-1D estimates against EC estimates for ET at the hourly timescale when considering Sites 6 (left) and 7 (right). R^2 is the determination coefficient, slope and offset result from linear regression between X and Y data (continuous line). Dotted line is the 1:1 line. The Nash coefficient is also reported.

When addressing the daily timescale, RMSE between EC and HYDRUS-1D estimates was 0.57 mm d^{-1} (33% relative) for Site 6, and 0.4 mm d^{-1} (18% relative) for Site 7, as displayed in Fig. 4. RMSE was stable throughout the simulation periods, which induced a larger RRMSE between August and December 2007 that depicted lower ET values, as compared to the [January–October] 2008 interval. Similar validation results were obtained when restricting the time interval to grapevine growth periods, with RMSE values of 0.62 mm d^{-1} (29% relative) and 0.49 mm d^{-1} (22% relative) for Site 6 and 7, respectively. The temporal dynamics of EC and HYDRUS-1D estimates of daily ET are displayed in Fig. 5 for Site 6 throughout the simulation period. This comparison was possible over Site 6 because the data collection was continuous throughout the experiment (Section 2.3). It is shown that HYDRUS-1D simulations and EC estimates depicted very similar temporal dynamics, for both dry and wet conditions. However, large differences were observed in September 2007 with an underestimation of EC estimates by HYDRUS-1D simulations during a very dry period, and in June 2008 with an overestimation of EC estimates by HYDRUS-1D simulations after heavy rainfall.

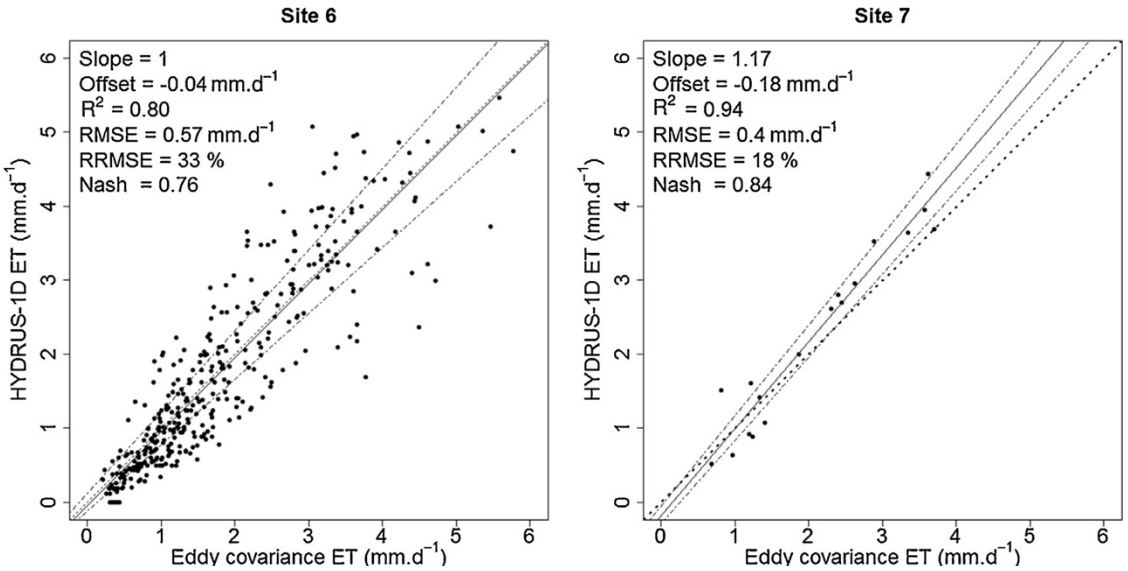

Fig. 4. Validation of HYDRUS-1D estimates against EC estimates for ET at the daily timescale when considering Sites 6 (left) and 7 (right). R^2 is the determination coefficient, slope and offset result from linear regression between X and Y data (continuous line). Dotted line is the 1:1 line. The Nash coefficient is also reported. Hyphen-dotted lines correspond to tolerance intervals given by ECPACK for EC estimates.

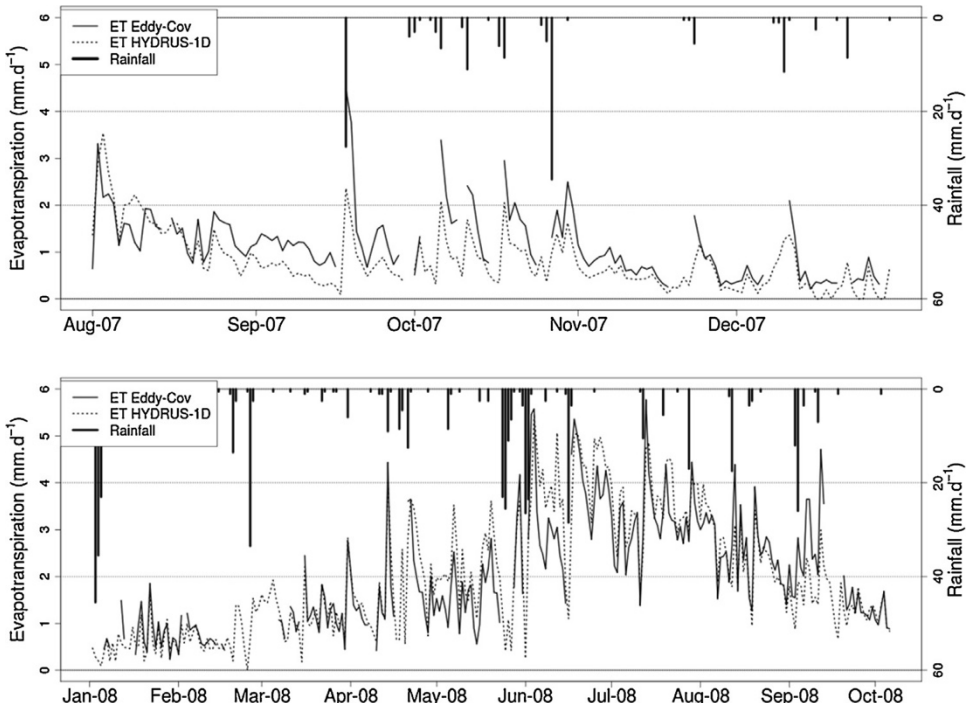

Fig. 5. Comparison of temporal dynamics for EC and HYDRUS-1D estimates of daily ET, for Site 6 throughout the experiment. Rainfall is also indicated (right-hand axis).

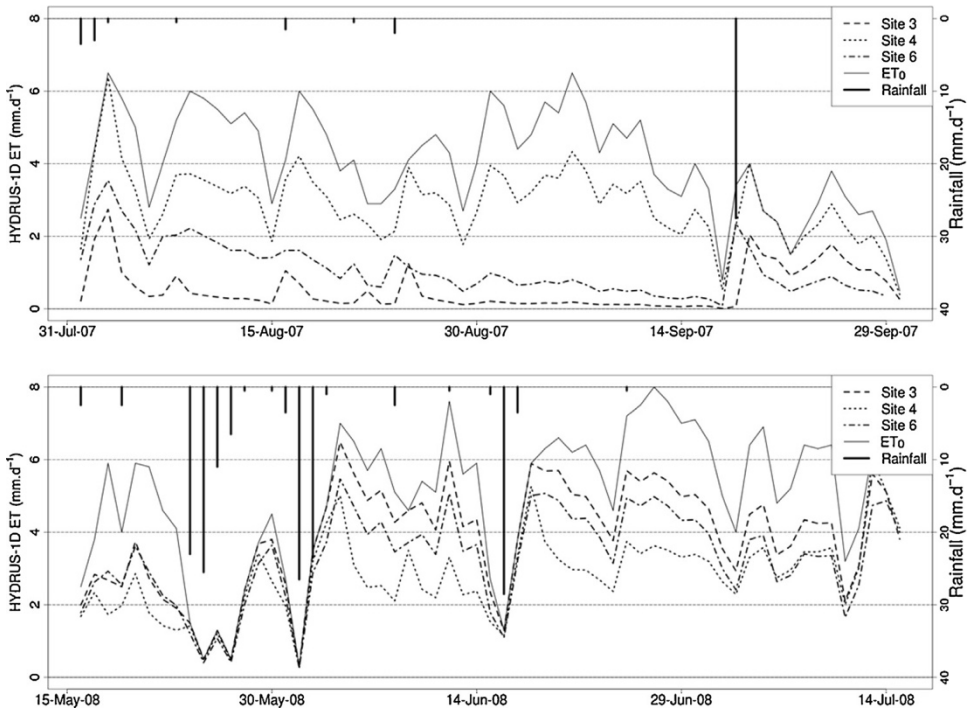

Fig. 6. Comparison of ET simulations from HYDRUS-1D for three sites that differed much in soil and water table conditions, when selecting (a) a dry period in 2007 and (b) a wet period in 2008 with significant rainfall. Short-grass reference evapotranspiration (ET_0) is also indicated.

4.3. Seasonal ET variability over study sites

When focusing on HYDRUS-1D estimates of daily ET throughout the simulation period, we observed large temporal dynamics for the seven sites, with seasonal variations of daily ET values between 0 and 6.5 mm d^{-1}. Further, the ET temporal dynamics differed much from one site to another, and we accordingly classified the seven sites into three groups. Group 1 included Sites 2 and 3 that experienced severe water stress during the end of summer (particularly in 2007 with daily ET values lower than 1 mm d^{-1}) and large evaporative rates during spring with ET values close to the short-grass reference evapotranspiration ET_0 after heavy rainfall (June 2008 with daily ET ranging between 4 and 6.5 mm d^{-1}). Group 2 included Sites 1, 6 and 7 that experienced water stress during the end of summer, with daily ET values around 1 mm d^{-1}, and constant evaporative rate for the rest of the simulation period. Group 3 included Sites 4 and 5 that depicted constant ET rates throughout the simulation period, with daily ET values between 2 and 4 mm d^{-1}, even during very dry periods.

The ET temporal dynamic is illustrated in Fig. 6 where three sites were selected as representative of each group above-listed. In this figure, we can identify severe water stresses during August and September 2007 for Site 3 (Group 1) with a low evaporative rate over more than 40 days. A similar dynamic was observed for Site 6 (Group 2) but for 10 days only during September 2007. Conversely, Site 4 (Group 3) continuously depicted an evaporative rate very close to ET_0 during the same period. We observed contrary situations for the same sites during a period of unrestrictive water availability in 2008 that followed heavy rainfall. Indeed, we observed large evaporative rates over short periods, particularly for Site 3 (Group 1), whereas ET for the three sites almost reached ET_0 after rainfall.

Cumulative statistics for the seven sites, as shown in Table 2, were consistent with the results discussed above. The three groups could be identified when considering cumulated ET during the full grapevine vegetation period, with Sites 2 and 3 (Group 1) depicting the lowest ET cumulated values; Sites 1, 6 and 7 (Group 2) depicting intermediate ET cumulated values; and Sites 4 and 5 (Group 3) depicting the largest ET cumulative values. For the driest and wettest sites, ET cumulated and daily values over full vineyard vegetation period showed large differences, with ET cumulated values of 255 mm and 565 mm, and ET daily value of 1.46 mm d^{-1} and 2.87 mm d^{-1}, which corresponded to a factor of two between these two sites.

Table 2. Statistics on HYDRUS-1D simulations of actual evapotranspiration ET over the seven study sites. Cumulated ET over the experimental period corresponds to cumulated ET from August 2007 to October 2008. Cumulated ET, averaged daily ET (Daily ET Mean), standard deviation on daily ET (daily ET STD) and coefficient of variation of daily ET (daily ET CV) for grapevine full vegetation period are statistical values obtained over both the [August 2007–October 2007] and the [June 2008-October 2008] periods.

Site	Experimental period	Grapevine full vegetation period (August 2007–October 2007; June 2008–October 2008)			
	Cumulated ET (mm)	Cumulated ET (mm)	Daily ET Mean (mm d^{-1})	Daily ET STD (mm d^{-1})	Daily ET CV (%)
Site 1	705	376	2.07	1.45	70
Site 2	805	339	1.87	1.01	54
Site 3	656	265	1.46	1.24	85
Site 4	791	522	2.87	1.09	38
Site 5	806	446	2.45	1.17	48
Site 6	689	361	1.98	1.37	69
Site 7	695	366	2.01	1.28	63

5. Discussion

The profile of calibration residual error, as expressed through RMSE between measured and simulated soil moisture profiles, was explained by the temporal dynamics of water fluxes within the unsaturated zone. Low RMSE values for deep layers were ascribed to slower exchanges related to drainage and capillary rises, whereas large RMSE values for root zone and soil surface were ascribed to faster exchanges related to plant transpiration and soil evaporation, respectively. The 10% overall RRMSE value between simulated and measured profiles was considered acceptable since the error on NP measurements was around 15% relative, while the RMSE values were similar to those reported in previous studies that addressed the performances of HYDRUS within irrigated and heterogeneous crops (Skaggs et al., 2004; Phogat et al., 2013, 2014). We explained the RMSE decrease during the simulation period by the stabilization of the numerical process, which justified the setting of a simulation starting date a few months before the measurements of soil moisture profiles (Section 3.2). The lack of an evident link between the RMSE values and the site features was consistent with the lack of systematic under/overestimation when analyzing the temporal dynamics of soil water storage from HYDRUS and EC estimates, which underlined the relevance of the proposed approach. Indeed, HYDRUS-1D calibration performances were similar throughout the simulation period and across a large range of grapevine water status, where both site and periods were typified by large differences in soil and/or water table conditions (Guix-Hébrard et al., 2007).

At the hourly timescale, the validation results for HYDRUS-1D estimates against EC estimates were similar to those reported in previous studies over irrigated vineyards (Ortega-Farias et al., 2007, 2010; Kool et al., 2014a), and the resulting accuracy on HYDRUS-1D

estimates was close to that regularly quoted for further applications (Seguin et al., 1999; Kalma et al., 2008). The same applied to the validation results at the daily timescale, with similar values as compared to those reported in previous studies over irrigated and rainfed vineyards (Trambouze et al., 1998; Bsaibes, 2007; Ortega-Farias et al., 2007, 2010), and with a resulting accuracy close to that required for further applications. This underlined the relevance of the proposed approach, since the validation relied on comparing two independent methods for ET estimation, i.e., the first one based on near surface turbulent fluxes (EC) and the second one based on water transfers in the unsaturated zone (HYDRUS-1D). An important outcome is that the calibration of HYDRUS-1D over times series of measured soil moisture profiles can be used as an alternative to EC measurements. Indeed, the approach based on HYDRUS-1D can assist in alleviating experimental efforts for device cost and maintenance, since measurements of soil moisture profile can be replicated across large spatial extents. This is all the more interesting that the considered study area depicts large heterogeneities in terms of pedology or water table dynamics (Guix-Hébrard et al., 2007) and in terms of canopy conditions such as row orientation, canopy thickness and inter-row weeding (Galleguillos et al., 2011a, 2011b).

When validating HYDRUS-1D estimates against EC estimates at both hourly and daily timescale, the larger differences we observed for Site 6 as compared to Site 7 was ascribed to the experimental conditions. Site 6 had a 0.15 km^2 size, and spread over nine fields including vineyards by 90% in surface area, whereas Site 7 had a 0.09 km^2 size and spread over one field only (Section 2.2). Besides, the EC footprint was designed in accordance to the site extent, since the measurement height for was larger (almost three times) for Site 6 than for Site 7. Therefore, the within-footprint variability in canopy conditions was larger for Site 6 as compared to Site 7, and the same applied for the within-footprint variability in evaporative rate.

The validation of HYDRUS-1D estimates at the hourly timescale showed large differences between model simulations and EC measurements during sunrise and sunset periods, which was consistent with the outcomes from Kool et al. (2014a) who reported a similar trend. This was ascribed to EC measurements that had difficulties in properly estimating evapotranspiration during sunrise and sunset periods, whereas several studies reported that energy balance fails under advection conditions (Rana and Katerji 2000; Zhang et al., 2008; Ding et al., 2015). However, these difficulties in estimating evapotranspiration were not considered critical, since they occurred during periods of low energy fluxes, with limited impacts at the daily timescale.

The three site groups we identified when analyzing the temporal dynamics of ET over the seven sites were not clearly correlated to the soil depth, soil texture and water table conditions. First, Group 1, 2 and 3 corresponded to shallow soils, shallow/deep soils, and deep soils, respectively. Second, Group 1 and 2 corresponded to absent/seasonal water tables, while Group 3 corresponded to seasonal/permanent water tables. Third, soil textures could be different within the same group (e.g., clay/gravels and silty/sandy for Group 1) or similar from one group to another (e.g., clay soils for Groups 1, 2 and 3). Therefore, we could not identify any evident link between ET temporal dynamics and soil depth/water table conditions, but a finer analysis required accounting for additional factors. Premature varieties might explain the large evaporative rates observed in spring 2008 for Sites 1, 3 and

6, whereas weeds were likely to induce ET values close to ET_0 after rainfall. For Site 3 with restrictive water availability, weeds might explain the larger values of daily ET as compared to Site 4 with a permanent water table. For Site 2, a premature variety might explain the large ET values in spring 2008 since there were no weeds. For Sites 4 and 5, the influence of a water table might explain the stable evaporative rates throughout the growth cycle, especially after a dry period in August and September 2007. Additionally, other factors such as farmer practices, including pruning or weeding, might have impacted on the temporal dynamics of evaporative rate, so that the ET rate was limited for the sites with water availability. For example, the pruning was necessary at Site 4, to prevent canopy vigor and thus obtain sufficient fruit quality.

6. Conclusions

The outcomes of the present studies are threefold. First, it was possible to calibrate HYDRUS-1D against measurements of soil moisture for a larger range of grapevine water status that resulted from very different soil and water table conditions. Second, HYDRUS-1D simulations after calibration can be used as an alternative to EC measurements within rainfed vineyards, to alleviate experimental efforts for device cost and maintenance, especially over a regional extent that depicts large heterogeneities in terms of pedology or water table conditions. Then, HYDRUS-1D simulations can be used for several applications such as characterizing spatial variabilities and temporal dynamics, assessing impact of pedological conditions and land use on evapotranspiration, or validating remote sensing retrievals over large regions. Third, HYDRUS-1D permitted the characterization of the temporal dynamics of evaporative rate over a large range of grapevine water status in space and time. It was possible to explain some coarse behaviors in relation to soil depth and water table conditions, but a finer analysis required accounting for additional factors such as variety precocity, weeds, as well as pruning and weeding practices that are necessary to ensure grape quality and yield.

Further investigations should focus on improving soil water balance modeling on several important issues related to soil conditions and vineyard structures. First, attention should be paid to non-equilibrium situations that are common for water fluxes within the vadose zone (Flury et al., 1994; Jarvis, 2007; Köhne et al., 2008), and that can be a source of error for both the calculation of water balance and the inverse estimation of soil hydrodynamic parameters. Besides, accounting for hysteresis effects is likely to assist in improving modeling and calibration for silty and clay soils (Fredlund et al., 2011; Osman, 2013). Second, a 2D model should be considered for including possible lateral water transfers and spatiotemporal differences in boundaries conditions (e.g., diurnal and seasonal courses of canopy shading effect within rows and inter-rows), which are key processes for row-structured canopies affecting the water balance in the soil (Ramos et al., 2012; Phogat et al., 2013, 2014; Kool et al., 2014a). Third, coupling the plant functioning and the soil water balance modeling should assist in better characterizing plant influences on water transfers, whereas the use of ancillary information about leaf area index is likely to improve the estimation of grapevine ET_0 (Allen et al., 2006). Then, the coupling with decision modeling would be valuable to account for farmer practices such as pruning and weeding.

Acknowledgments

The authors thank the LISAH technical staff for the experiment. This study benefited from grants by the Chilean National Commission for Scientific and Technological Research, and by the French National Institute for Agricultural Research. M. Galleguillos acknowledges the support of Project CONICYT/FONDAP/1511000. The authors are grateful to the Editorial Review Board of the Agricultural Water Management Journal who helped to improve the manuscript.

References

Simunek, J., Hopmans, J.W., 2009. Modeling compensated root water and nutrient uptake. Ecol. Modell. 220, 505–521.

Simunek, J., van Genuchten, M. Th., Sejna, M., 2016. Recent developments and applications of the HYDRUS computer software packages. Vadose Zone J. 15 (7), 25.

Allen, R., Pereira, L., Raes, D., Smith, M., 1998. Crop Evapotranspiration. Guideline for Computing Crop Water Requirements. FAO Irrigation Drainage Paper No 56. FAO, Roma, Italia.

Allen, R., Pereira, L., Raes, D., Smith, M., 2006. Evapotranspiración del Cultivo. Guías para la determinación de los requerimientos de agua de los cultivos. Serie Riego y Drenaje, 56. Estudio FAO, Roma, pp. 298.

Arbat, G., Puig-Barguéz, J., Duran-Ros, M., Barragan, J., Ramírez de Cartagena, F., 2013. Drip Irriwater: computer software to simulate soil-wetting patterns under surface drip irrigation. Comput. Electron. Agric. 98, 183–192.

Bsaibes, A., 2007. Évaluation d'une approche multi-locale d'estimation spatiale de l'évapotranspiration. PhD thesis. Université de Montpellier II.

Ding, R., Kang, S., Zhang, Y., Hao, X., Tong, L., Li, S., 2015. A dynamic surface conductance to predict crop water use from partial to full canopy cover. Agric. Water Manage. 150, 1–8.

Dobriyal, P., Qureshi, A., Badola, R., Hussain, S.A., 2012. A review of the methods available for estimating soil moisture and its implications for water resource management. J. Hydrol. 458–459, 110–117.

Feddes, R.A., Kowalik, P.J., Zaradny, H., 1978. Simulation of field water use and crop yield. In: Simulation Monographs. PUDOC, Wageningen (189pp).

Flury, M., Fluhler, H., Jury, A., Leuenberger, J., 1994. Susceptibility of soil to preferential flow of water: a field study. Water Resour. Res. 30, 1945–1954.

Fredlund, D.G., Sheng, D., Zhao, D., 2011. Estimation of soil suction from the soil-water characteristic curve. Canadian Geotechnical Journal 48, 186–198.

Galleguillos, M., Jacob, F., Prévot, L., Lagacherie, P., Liang, S., 2011a. Mapping daily evapotranspiration over a Mediterranean vineyard watershed. IEEE Geosci. Remote Sens. Lett. 99, 168–172.

Galleguillos, M., Jacob, F., Prévot, L., French, A., Lagacherie, P., 2011b. Comparison of two temperature differencing methods to estimate daily evapotranspiration over a Mediterranean vineyard watershed from ASTER data. Remote Sens. Environ.115(6),1326–1340.

Griesser, M., Weingart, G., Shoedl-Hummel, K., Neumann, N., Becker, M., Varmuza, K., Liebner, F., Schuhmacher, R., Forneck, A., 2015. Severe drought stress is affecting selected primary metabolites, polyphenols, and volatile metabolites in grapevine leaves (Vitis Vinifera cv. Pinot noir). Plant Physiol. Biochem. 88, 17–26.

Guix-Hébrard, N., Voltz, M., Trambouze, W., Gaudillère, J.P., Lagacherie, P., 2007. Influence of water table depths on the variation of grapevine water status at the landscape scale. Eur. J. Agron. 27 (2–4), 187–196.

Heilman, J.L., McInnes, K.J., Savage, M.J., Gesch, R.W., Lascano, R.J., 1994. Soil and canopy energy balances in a west Texas vineyard. Agric. Forest Meteorol. 71 (1–2), 99–114.

Heilman, J.L., McInnes, K.J., Gesch, R.W., Lascano, R.J., Savage, M.J., 1996. Effects of trellising on the energy balance of a vineyard. Agric. Forest Meteorol. 81 (1), 79–93.

Horst, T., Weil, J., 1992. Footprint estimation for scalar flux measurements in the atmospheric surface-layer. Boundary Layer Meteorol. 59 (3), 279–296.

Jarvis, N., 2007. A review of non-equilibrium water flow and solute transport in soil macropores: principles, controlling factor and consequences for water quality. Eur. J. Soil Sci. 58, 523–546.

Köhne, J.M., Köhne, S., Simunek, J., 2008. A review of model applications for structured soils: a) Water flow and tracer transport. J. Contam. Hydrol. 104, 4–35.

Kaimal, J.C., Finnigan, J.J., 1994. Atmospheric Boundary Layer Flows, Their Structure and Measurement. Oxford University Press(289pp).

Kalma, J.D., McVicar, T.R., McCabe, M.F., 2008. Estimating land surface evaporation: a review of methods using remotely sensed surface temperature data. Surv. Geophys. 29 (4–5), 421–469.

Kandelous, M., Simunek, J., 2010. Numerical simulations of water movement in a subsurface drip irrigation system under field and laboratory conditions using HYDRUS-2D. Agric. Water Manage. 97, 1070–1076.

Kandelous, M.M., Kamai, T., Vrugt, J.A., Simunek, J., Hanson, B., Hopmans, J.W., 2012. Evaluation of subsurface drip irrigation design and management parameters for alfalfa. Agric. Water Manage. 109, 81–93.

Kool, D., Ben-Gal, A., Agam, N., Simunek, J., Heitman, L., Sauer, T.J., Lazarovitch, N., 2014a. Spatial and diurnal below canopy evaporation in a desert vineyard: measurements and modeling. Water Resour. Res. 50, 7035–7049.

Kool, D., Agam, N., Lazarovitch, N., Heitman, J.L., Sauer, T.J., Ben-Gal, A., 2014b. A review of approaches for evapotranspiration partitioning. Agric. Forest Meteorol. 184, 56–70.

Lereboullet, A.-L., Beltrando, G., Bardsley, D.K., 2013. Socio-ecological adaptation to climate change: a comparative case study from the Mediterranean wine industry in France and Australia Agriculture. Ecosyst. Environ. 164, 273–285.

Li, S., Kang, S., Li, F., Zhang, L., Zhang, B., 2008. Vineyard evaporative fraction based on eddy covariance in an arid desert region of northwest china. Agric. Water Manage. 95 (8), 937–948.

Li, S., Tong, L., Li, F., Zhang, L., Zhang, B., Kang, S.,2009. Variability in energy partitioning and resistance parameters for a vineyard in northwest china. Agric. Water Manage. 96 (6), 955–962.

Liang, N.-N., Zhu, B.-Q., Han, S., Wang, J.-H., Pan, Q.-H., Reeves, M.J., Duan, C.-Q., He, F., 2014. Regional characteristics of anthocyanin and flavonol compounds from grapes of four Vitis Vinifera varieties in five wine regions of China. Food Res. Int. 64, 264–274.

Montes, C., Jacob, F., 2016. Comparing Landsat-7 ETM+ and ASTER Imageries to Estimate Daily Evapotranspiration Within a Mediterranean Vineyard Watershed. Geoscience and Remote Sensing Letters (in revisions).

Montes, C., Lhomme, J.P., Demarty, J., Prévot, L., Jacob, F., 2014. A three-source SVAT modeling of evaporation: application to the seasonal dynamics of a grassed vineyard. Agric. Forest Meteorol. 191, 64–80.

Neuman, S., Feddes, R., Bresler, E., 1974. Finite Element Simulation of Flow in Saturated-unsaturated Soils Considering Water Uptake by Plants. Tech. Rep., Third Annual Report, Project No. A10-SWC-77.

OIV, 2007. Structure of the World Vitivinicultural Industry in 2007. Organisation Internationale de la Vigne et du Vin (Available at:) http://www.oiv.int.

Ortega-Farias, S., Carrasco, M., Olioso, A., Acevedo, C., Poblete, C., 2007. Latent heat flux over cabernet sauvignon vineyard using the Shuttleworth and Wallace model. Irrig. Sci. 25 (2), 161–170.

Ortega-Farias, S., Poblete-Echeverria, C., Brisson, N., 2010. Parameterization of a two layer model for estimating vineyard evapotranspiration using meteorological measurements. Agric. Forest Meteorol. 150, 276–286.

Osman, K., 2013. Soil water, irrigation and drainage. In: Soils: Principles, Properties and Management. Springer, Netherlands, pp. 67–88 (263 pp.).

Patel, N., Rajput, T.B.S., 2008. Dynamics and modeling of soil water under subsurface drip irrigated onion. Agric. Water Manage. 95, 1335–1349.

Pellegrino, A., Lebon, E., Simmoneau, J., Wery, J., 2005. Towards a simple indicator of water stress in grapevine (Vitis Vinifera l.) based on the differential sensitivities of 18 vegetative growth components. Aust. J. Grape Wine Res. 11, 306–315.

Pellegrino, A., Goze, E., Lebon, E., Wery, J., 2006. A model-based diagnosis tool to evaluate the water stress experienced by grapevine in field sites. Eur. J. Agron. 25 (1), 49–59.

Phogat, V., Skewes, M.A., Cox, J.W., Alam, J., Grigson, G., Simunek, J.,2013. Evaluation of water movement and nitrate dynamics in a lysimeter planted with an orange tree. Agric. Water Manage. 127, 74–84.

Phogat, V., Skewes, M., Cox, J., Sanderson, G., Alam, J., Simunek, J., 2014. Seasonal simulation of water, salinity and nitrate dynamics under drip irrigated mandarin (Citrus reticulata) and assessing management options for drainage and nitrate leaching. J. Hydrol. 513, 504–516.

Ramos, T.B., Simunek, J., Goncalves, M.C., Martins, J.C., Prazeres, A., Castanheira, N.L., Pereira, L.S., 2011. Field evaluation of a multicomponent solute transport model in soils irrigated with saline waters. J. Hydrol. 407, 129–144.

Ramos, T.B., Simunek, J., Goncalves, M.C., Martins, J.C., Prazeres, A., Pereira, L.S., 2012. Two-dimensional modeling of water and nitrogen fate from sweet sorghum irrigated with fresh and blended saline waters. Agric. Water Manage. 111, 87–104.

Rana, G., Katerji, N., 2000. Measurement and estimation of actual evapotranspiration in the field under Mediterranean climate: a review. Eur. J. Agron. 13 (2–3), 125–153.

Richards, L., 1931. Capillary conduction of liquids through porous media. Physics 1, 318–333.

Riou, C., Pieri, P., Clech, B.L., 1994. Consommation d'eau de la vigne en conditions hydriques non limitantes. Formulation simplifiée de la transpiration. Vitis 33, 109–115.

Seguin, B., Becker, F., Phulpin, T., Guyot, G., Kerr, Y., 1999. IRSUTE: a minisatellite project for land surface heat flux estimation from field to regional scale. Remote Sens. Environ. 68, 357–369.

Sene, K.J., 1994. Parameterisations for energy transfers from a sparse vine crop. Agric. Forest Meteorol. 71 (1–2), 1–18.

Skaggs, T.H., Trout, T.J., Simunek, J., Shouse, P.J., 2004. Comparison of HYDRUS-2D simulations of drip irrigation with experimental observations. J. Irrig. Drain. Eng. 130, 304–310.

Smart, R., 1973. Sunlight interception by vineyards. Am. J. Enol. Vitic. 24, 141–147.

Spano, D., Snyder, R.L., Duce, Paw., 2000. Estimating sensible and latent heat flux densities from grapevine canopies using surface renewal. Agric. Forest Meteorol. 104 (3), 171–183.

Tóth, J.P., Végvári, Z., 2016. Future of wine grape growing regions in Europe. Aust. J. Grape Wine Res. 22, 64–72.

Trambouze, W., Voltz, M., 2001. Measurement and modelling of the transpiration of a Mediterranean vineyard. Agric. Forest Meteorol.107(2),153–166.

Trambouze, W., Bertuzzi, P., Voltz, M., 1998. Comparison of methods for estimating actual evapotranspiration in a row-cropped vineyard. Agric. Forest Meteorol. 91 (3–4), 193–208.

Trambouze, W., 1996. Caractérisation Et éléments De Modélisation De l'évapotranspiration réelle De La Vigne à l'échelle De La Parcelle. Ph.D. Thesis. ENSAM, INRA.

Valiantzas, J.D., 2006. Simplified versions for the penman evaporation equation using routine weather data. J. Hydrol. 331 (3–4), 690–702.

Verstraeten, W.W., Veroustraete, F., Feyen, J., 2008. Assessment of evapotranspiration and soil moisture content across different scales of observation. Sensors 8, 70–117.

Vrugt, J.A., van Wijk, M.T., Hopmans, J.W., Simunek, J., 2001. One-, two-and three-dimensional root water uptake functions for transient modelling. Water Resour. Res. 37, 2457–2470.

Wesseling, J., 1991. Meerjarige Simulaties Van Grondwateronttrekking Voor Verschillende Bodemprofielen, Grondwatertrappen En Gewassen Met Het Model SWATRE Rep. 152. Tech. Rep. Winand Staring Centre, Wageningen, the Netherlands.

Yunusa, I.A.M., Walker, R.R., Lu, P., 2004. Evapotranspiration components from energy balance: sapflow and microlysimetry techniques for an irrigated vineyard in inland Australia. Agric. Forest Meteorol. 127, 93–107.

Zahavi, T., Reuveni, M., Scheglov, D., Lavee, S., 2001. Effect of grapevine training systems on development on powdery mildew. Eur. J. Plant Pathol. 107, 495–501.

Zarco-Tejada, P., Berjon, A., Lopez-Lozano, R., Miller, J., Martin, P., Cachorro, V., González, M.R., de Frutos, A., 2005. Assessing vineyard condition with hyperspectral indices: leaf and canopy reflectance simulation in a row-structured discontinuous canopy. Remote Sens. Environ. 99 (3), 271–287.

Zhang, B., Kang, S., Li, F., Zhang, L., 2008. Comparison of three evapotranspiration models to Bowen ratio-energy balance method for a vineyard in an arid desert region of northwest China. Agric. Forest Meteorol. 148, 1629–1640.

Zitouna-Chebbi, R., Prévot, L., Jacob, F., Mougou, R., Voltz, M., 2012. Assessing the consistency of eddy covariance measurements under conditions of sloping topography within a hilly agricultural catchment. Agric. Forest Meteorol. 164, 123–135.

Zitouna-Chebbi, R., Prévot, L., Jacob, F., Voltz, M., 2015. Accounting for vegetation height and wind direction to correct eddy covariance measurements of energy fluxes over hilly crop fields. J. Geophys. Res. – Atmos. 120, 4920–4936.

van Dijk, A., Moene, A.F., de Bruin, H.A.R., 2004. The Principle of Surface Flux Physics: Theory, Practice and Description of the ECPACK Library. Tech. Rep., Internal Report 2004/1. Meteorology and Air Quality Group, Wageningen University Wageningen, The Netherlands (99p).

van Genuchten, M.Th., 1980. A closed-form equation for predicting the hydraulic conductivity of unsaturated soils. Soil Sci. Soc. Am. J. 44, 892–898.